Contribution from the Departments of Chemistry, University of Massachusetts, Amherst, Massachusetts 01003, University of Minnesota, Minneapolis, Minnesota 55455, and Iowa State University, Ames, Iowa 50010

X-ray Absorption Spectroscopic Studies of the Sulfide Complexes of Hemerythrin

Michael J. Maroney,*[,†] Robert C. Scarrow,[‡] Lawrence Que, Jr.,*[,‡] A. Lawrence Roe,[‡] Gudrun S. Lukat,[§] and Donald M. Kurtz, Jr.[§,∥]

Received July 22, 1988

The structures of the dinuclear iron sites of (μ-sulfido)methemerythrin and (μ-sulfido)semi-methemerythrin are explored by using X-ray absorption spectroscopy. The analysis of pre-edge features in the XAS spectrum of (μ-S)metHr does not reveal a significant change in the coordination number/geometry of the iron centers compared with those of native oxo/hydroxo-bridged forms of the protein. The EXAFS analysis of the first coordination sphere data is consistent with the expected five- and six-coordination of the iron atoms and with the presence of a sulfido bridge, with an average Fe-S distance of 218 pm. The Fe-Fe distance in (μ-S)metHr is found to be 335 pm. Upon reduction of the protein to (μ-S)semi-metHr, the Fe-Fe distance lengthens to 359 pm, while the Fe-S distance remains unchanged. Lengthening of the Fe-Fe distance and the average Fe-O,N bond distance upon reduction is shown to be relevant to structural changes that occur upon reduction of the native oxo/hydroxo-bridged forms of the protein and the interconversion between two distinct forms of semi-metHr, (semi-met)$_r$Hr and (semi-met)$_o$Hr. The larger bridging sulfide apparently favors an iron site structure resembling that of (semi-met)$_o$Hr.

Introduction

Proteins containing dinuclear iron active sites can be grouped into two general classes. The first class, typified by plant ferredoxins, contain two antiferromagnetically coupled tetrahedral iron centers bridged by two sulfides.[1] The remaining two sites on each iron are usually occupied by cysteine thiolates, although histidine is believed to substitute for two of the four cysteinates in Rieske centers.[2] The second class consists of proteins with five- or six-coordinate iron centers antiferromagnetically coupled via an oxo or hydroxo bridge and bound to the protein by O- and N-donor atoms of amino acid side chains. The active site of the respiratory protein hemerythrin (Hr) is archetypical of this structural class, which also includes ribonucleotide reductase,[3] uteroferrin and purple acid phosphatases,[4] and methane monooxygenase.[5]

The dinuclear iron site of Hr has been studied in three different oxidation states, metHr and oxyHr (Fe^{III}_2), semi-metHr ($Fe^{III}Fe^{II}$), and deoxyHr (Fe^{II}_2), by employing a wide variety of physical techniques.[6] The structures of diferric forms of the protein are characterized in the most detail, since several crystal structures of these forms are now available.[7] As illustrated by **1** (for

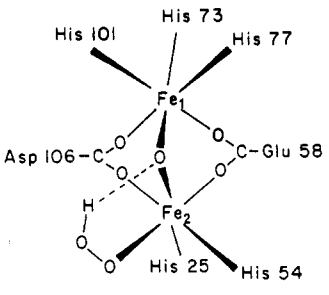

1

oxyhemerythrin), these studies reveal that the iron atoms are bound to the protein by five histidines (three to one iron atom, Fe_1, and two to the other, Fe_2) and two bridging carboxylate groups from aspartate and glutamate residues. In addition, an oxo bridge is present, which gives rise to the observed antiferromagnetic coupling ($J = -134$ cm^{-1} in metHr) of the high-spin ferric centers. EXAFS spectroscopic studies,[3a,8] along with NMR[9] and MCD[10] investigations designed to probe magnetic interactions, reveal that these essential features are retained in various semi-metHr forms and in deoxyHr, except that the oxo bridge is protonated to form a hydroxo bridge between the iron atoms upon reduction by one or two electrons.

All three oxidation levels of Hr will bind small anions to form complexes, involving the addition of the anion to a vacant coordination site (or displacement of an aquo ligand) on Fe(2).[6a,9,10] In contrast to the simple coordination characteristic of anions such as azide, sulfide (or hydrosulfide) reacts with metHr to first reduce the dinuclear cluster to the semi-met level and is then incorporated into the cluster to form (μ-sulfido)semi-methemerythrin ((μ-S)-semi-metHr) as evidenced by its unique EPR, electronic absorption, resonance Raman, and Mössbauer spectroscopic features.[11] This novel dinuclear site can be oxidized to (μ-sulfido)methemerythrin ((μ-S)metHr), which retains LMCT transitions characteristic of Fe,S proteins and has a resonance Raman spectrum consistent with the replacement of the oxo bridge by sulfide.[12]

The incorporation of sulfide into the dinuclear cluster dramatically alters the chemistry of the site. The reduction potential for the met to semi-met interconversion is raised, and the fully

† University of Massachusetts.
‡ University of Minnesota.
§ Iowa State University.
∥ Current address: Department of Chemistry, University of Georgia, Athens, GA 30602.

(1) Berg, J. M.; Holm, R. H. *Met. Ions Biol.* **1982**, *4*, (Chapter 1).
(2) (a) Telser, J.; Hoffman, B. M.; LoBrutto, R.; Ohnishi, T.; Tsai, A.-L.; Simpkin, D.; Palmer, G. *FEBS Lett.* **1987**, *214*, 117-121. (b) Cline, J. F.; Hoffman, B. M.; Mims, W. B.; LaHaie, E.; Ballou, D. P.; Fee, J. A. *J. Biol. Chem.* **1985**, *260*, 3251-3254. (c) Kuila, D.; Fee, J. A.; Schoonover, J. R.; Woodruff, W. H.; Batie, C. J.; Ballou, D. P. *J. Am. Chem. Soc.* **1987**, *109*, 1559-1561.
(3) (a) Scarrow, R. C.; Maroney, M. J.; Palmer, S. M.; Que, L., Jr.; Roe, A. L. *J. Am. Chem. Soc.* **1987**, *109*, 7857-7864. (b) Scarrow, R. C.; Maroney, M. J.; Palmer, S. M.; Que, L., Jr.; Salowe, S. P.; Stubbe, J. *J. Am. Chem. Soc.* **1986**, *108*, 6832-6834. (c) Sjöberg, B.-M.; Gräslund, A. *Adv. Inorg. Biochem.* **1983**, *5*, 87-110.
(4) (a) Averill, B. A.; Davis, J. C.; Burman, S.; Zirino, T.; Sanders-Loehr, J.; Loehr, T. M.; Sage, J. T.; Debrunner, P. G. *J. Am. Chem. Soc.* **1987**, *109*, 3760-3767. (b) Kauzlarich, S. M.; Teo, B. K.; Zirino, T.; Burman, S.; Davis, J. C.; Averill, B. A. *Inorg. Chem.* **1986**, *25*, 2781-2785. (c) Antanaitis, B. C.; Aisen, P. *Adv. Inorg. Biochem.* **1983**, *5*, 111-136. (d) Davis, J. C.; Averill, B. A. *Proc. Natl. Acad. Sci. U.S.A.* **1982**, *79*, 4623-4627.
(5) (a) Ericson, A.; Hedman, B.; Hodgson, K. O.; Green, J.; Dalton, H.; Bentsen, J. G.; Beer, R. H.; Lippard, S. J. *J. Am. Chem. Soc.* **1988**, *110*, 1996-1997. (b) Prince, R. C.; George, G. N.; Savas, J. C.; Cramer, S. J.; Patel, R. N. *Biochim. Biophys. Acta* **1988**, *952*, 220-229. (c) Woodland, M. P.; Dalton, H. *J. Biol. Chem.* **1984**, *259*, 53-59.
(6) (a) Wilkins, P. C.; Wilkins, R. G. *Coord. Chem. Rev.* **1987**, *79*, 195-214. (b) Klotz, I. M.; Kurtz, D. M., Jr. *Acc. Chem. Res.* **1984**, *17*, 16-22. (c) Wilkins, R. G.; Harrington, P. C. *Adv. Inorg. Biochem.* **1983**, *5*, 51-85. (d) Sanders-Loehr, J.; Loehr, T. M. *Adv. Inorg. Biochem.* **1979**, *1*, 235-252.
(7) (a) Stenkamp, R. E.; Sieker, L. C.; Jensen, L. H. *J. Am. Chem. Soc.* **1984**, *106*, 618-622. (b) Hendrickson, W. A. In *Invertebrate Oxygen-Binding Proteins: Structure, Active Site and Function*; Lamy, J., Lamy, J., Eds.; Marcel Dekker: New York, 1981; pp 503-515.
(8) Elam, W. T.; Stern, E. A.; McCallum, J. D.; Sanders-Loehr, J. *J. Am. Chem. Soc.* **1982**, *105*, 1919-1923.
(9) Maroney, M. J.; Kurtz, D. M., Jr.; Nocek, J. M.; Pearce, L. L.; Que, L., Jr. *J. Am. Chem. Soc.* **1986**, *108*, 6871-6879.
(10) Reem, R. C.; Solomon, E. I. *J. Am. Chem. Soc.* **1987**, *109*, 1216-1226.
(11) (a) Freier, S. M.; Duff, L. L.; Van Duyne, R. P.; Klotz, I. M. *Arch. Biochem. Biophys.* **1980**, *205*, 449-463. (b) Kurtz, D. M., Jr.; Sage, J.-T.; Hendrich, M.; Debrunner, P. G.; Lukat, G. S. *J. Biol. Chem.* **1983**, *258*, 2115-2117.
(12) Lukat, G. S.; Kurtz, D. M., Jr.; Shiemke, A. K.; Loehr, T. M.; Sanders-Loehr, J. *Biochemistry* **1984**, *23*, 6416-6422.

0020-1669/89/1328-1342$01.50/0

reduced cluster is rendered inaccessible.[13] Another effect is that the cluster no longer adds azide and other anions in either oxidation level. These changes in chemistry and the associated spectral features of the sulfide complexes are reminiscent of Fe,S proteins, particularly Rieske centers, and suggest that the sulfide complexes of Hr represent a link between the two classes of dinuclear iron proteins that may prove to be useful in understanding the properties associated with the different structures. In addition, the fact that the sulfide complexes of Hr can be prepared in both diferric and mixed-valence forms provides an opportunity to examine structural differences between the two oxidation levels. We report here the results of an X-ray absorption spectroscopic (XAS) study of the structure of sulfide complexes of metHr and semimetHr.

Experimental Section

Samples of (μ-S)semi-metHr were prepared by the addition of NaHS solution to a solution of metHr, obtained from *Phascolopsis gouldii* oxyHr, in Tris–perchlorate buffer (pH = 8.0) as previously described.[13] The sample used for the EXAFS studies was concentrated in a membrane concentrator in an N_2-filled glovebag. The final concentration of 7.5 mM in dinuclear iron sites was determined by integration of the (μ-S)semimetHr EPR signal. Little, if any, decomposition was noted following exposure to synchrotron radiation: the exposed sample retained 93% of the EPR signal obtained from the unexposed sample.

Samples of (μ-S)metHr were prepared from (μ-S)semi-metHr in 20 mM Tris buffer (pH = 8.0) by dialysis against a 3 mM solution of $K_3Fe(CN)_6$.[13] The sample was subsequently concentrated to ca. 9 mM. No significant decomposition from exposure to synchrotron radiation was noted by a comparison of the absorption spectra of unexposed and exposed samples.

Fluorescence data were taken on the protein samples with a large solid angle detector[14] using a Mn filter and Soller slits. The data were collected at station C-2 of the Cornell High Energy Synchrotron Source (CHESS) using a Si(111) double-crystal monochromator, which was detuned by 50% to improve harmonic rejection. The samples were frozen in sample holders and held in thermal contact with liquid nitrogen in a cryostat. Data on the model compounds $Fe(ddtc)_3$, $(Et_4N)_2[Fe_4S_4Cl_4]$, and $(Me_4N)_2[Fe_4S_4(SPh)_4]$ were collected in the transmission mode on powdered samples, diluted with boron nitride, at room temperature at station A-3 of CHESS. The monochromators were calibrated by using the 7113.0-eV 1s $\rightarrow$ 3d peak in the XAS spectrum of $Et_4N[FeCl_4]$ suspended in Duco cement, as previously described.[3a]

The pre-edge regions of the XAS spectra of (μ-S)metHr and metHrN_3 were analyzed by a procedure that involves normalization of the edge jump followed by subtraction of the background and edge region with a function composed of linear and arctangent components.[15] EXAFS data reduction and least-squares fits were performed as described elsewhere in detail.[3a] Initial fits were generated by using Fourier-filtered data. The results of these fits were used as initial parameters in refinements with the unfiltered data. In fits to Fourier-filtered data, the calculated spectrum and the data were both Fourier-transformed over the same limits in order to minimize the effects of truncation artifacts. Least-squares refinements employed k^3-weighted EXAFS data and minimized $R = [\sum k^6(\chi_c - \chi)^2/n]^{1/2}$, where the summation is performed over the n data points collected between 0.04 and 0.14 pm^{-1}. Although the data beyond k = 0.11 pm^{-1} becomes quite noisy, the higher k data were included in order to maximize the contribution of high-Z scattering atoms (i.e. Fe and S) in the EXAFS spectra. Fits obtained from data truncated at k = 0.11 pm^{-1} did not exhibit substantial differences in the distances found for various absorber–scatterer pairs or in the number of scattering atoms involved. For the analysis of Fourier-filtered EXAFS, back-transform windows of 110–230 and 240–410 pm were employed to isolate the EXAFS arising from the scattering atoms in the first coordination sphere and those in the second and third coordination spheres, respectively. Our analyses of EXAFS arising from a single shell of scattering atoms employ the theoretical functions of Teo and Lee,[16] plus two empirical parameters obtained from model compounds: A, an amplitude reduction factor, and ΔE, the edge shift. The values of the empirical parameters used for O, N, and Fe scatterers were the same parameters used in an earlier study of dinuclear Fe proteins,[3a] and parameters for S scatterers were obtained as discussed below. Because large correlations exist between the number of scatterers, N, and the Debye–Waller parameter, σ^2 (static and dynamic disorder), and between r and ΔE, we have employed our restricted-fit protocol[3a] in the analysis of the EXAFS of (μ-S)metHr and (μ-S)semi-metHr. This method restrains the value of N in cases where it has narrow limits (such as in the first coordination sphere) to integer values for a given refinement and allows the disorder factor to be adjusted. In cases where N is less well defined, σ^2 is held at a value determined from models and N is allowed to vary. In addition, ΔE for a given shell of scattering atoms is not varied during refinement. Thus, only two parameters per shell are allowed to vary in a given refinement, either r and σ^2 or r and N.

Previous work[3a] has indicated that although the EXAFS arising from mixed O,N-scatterers at ca. 200 pm in various structurally characterized models of hemerythrin can be fit with a single shell of O- or N-scatterers, attempts to fit the data using only oxygen or nitrogen parameters lead to systematic errors in the average bond length of the first-coordination-sphere scattering atoms and often give unreasonable values of N (or σ^2). These effects can be traced to the presence of interference in the EXAFS arising from O-donors (carboxylates) and N-donors (histidines) that feature different, but unresolvable, Fe–L distances. Fits that better approximate the average first-coordination-sphere O,N bond length can be obtained when a mixed shell is used. In order to avoid introducing more adjustable parameters, constraints on r and σ^2 are made such that $r_N = r_O + 12$ pm and $\sigma^2_N = \sigma^2_O$. Thus, the adjusted parameters of the O- and N-scatterers are bound to each other. This approach was also used in modeling the first coordination sphere of (μ-S)metHr and (μ-S)semi-metHr in this work, in order to allow a direct comparison with the results on other forms of hemerythrin to be made.

The values of A, ΔE, and σ^2 employed in the analysis of EXAFS arising from C, N, O, and Fe scattering atoms in (μ-S)metHr and (μ-S)semi-metHr were taken from previously reported model data.[3a] These parameters were determined for an Fe–S absorber–scatterer pair by analysis of the EXAFS of $Fe(ddtc)_3$ at room temperature. This compound is a desirable model in that it contains six identical sulfur atoms in the first coordination sphere. However, it is a known case of spin-state equilibrium, with crystal structures and magnetic susceptibility data indicating that the room-temperature form is high-spin Fe(III) (average Fe–S = 235.7 (3) pm at 297 K), while the low-temperature form is low spin (average Fe–S = 230.6 (1) pm at 79 K).[17] The results of best fit based on theory (BFBT) analysis[18] of the room-temperature EXAFS indicate that the form studied at room temperature was the *low-spin* form. A value of r = 230.5 (3) pm with ΔE = −4.2 (5) eV, A = 0.48 (2), and σ^2 = 78 (3) pm^2 (R = 0.40) was obtained from BFBT analysis. A transfer of parameters adopted from fits of $Fe(ddtc)_3$ (A = 0.44, ΔE = −4 eV) to model the first-coordination-sphere EXAFS of $(Et_4N)_2[Fe_4S_4Cl_4]$ and $(Me_4N)_2[Fe_4S_4(SPh)_4]$ by varying only r and σ^2 led to values of r = 224.3 (1) pm for the average Fe–S,Cl distance (crystal structure 226.6 (3) pm)[19] in the first compound and r = 225.6 (1) pm for the average Fe–S distance (crystal structure 227.9 (4) pm)[20] in the second compound with σ^2 and R values of 34 pm^2, 0.63 and 30 pm^2, 0.58, respectively. On the basis of these fits, the parameters were shown to give good bond lengths and reasonable values of σ^2 and were adopted for use in the analysis of the (μ-S)metHr and (μ-S)semi-metHr spectra. Apparently, grinding the sample of $Fe(ddtc)_3$ induces a spin-state change, as has been known to occur in other compounds.[21]

The errors indicated between the EXAFS fits using single-scattering theory and the values obtained from crystallography represent good estimates of the errors in the distances involving first-coordination-sphere scattering atoms (ca. 2 pm). This is the same value previously obtained for O,N scattering atoms from the analysis of structurally characterized hemerythrin models.[3a] These models also yield estimated errors of ca. ±3 pm for the Fe–Fe distance.

Results and Discussion

I. (μ-S)metHr. A. Analysis of Pre-Edge Features. The pre-edge and edge regions of an X-ray absorption spectrum contain features that arise from transitions of metal core electrons into higher energy bound or continuum states. In the case of high-spin ferric complexes, a small pre-edge peak at 7114 eV has been attributed to a 1s $\rightarrow$ 3d electronic transition. This transition is symmetry forbidden in centrosymmetric point groups and therefore increases in area in the order six-coordinate < five-coordinate < four-coordinate (tetrahedral), as the structure of the

(13) Lukat, G. S.; Kurtz, D. M., Jr. *Biochemistry* **1985**, *24*, 3464–3472.
(14) Stern, E. A.; Heald, S. M. *Rev. Sci. Instrum.* **1979**, *50*, 1579–1582.
(15) Roe, A. L.; Schneider, D. J.; Mayer, R. J.; Pyrz, J. W.; Widom, J.; Que, L., Jr. *J. Am. Chem. Soc.* **1984**, *106*, 1676–1681.
(16) Teo, B. K.; Lee, P. A. *J. Am. Chem. Soc.* **1979**, *101*, 2815–2832.
(17) Leipoldt, J. G.; Coppens, P. *Inorg. Chem.* **1973**, *12*, 2269–2274.
(18) Teo, B. K.; Antonio, M. R.; Averill, B. A. *J. Am. Chem. Soc.* **1983**, *105*, 3751–3762.
(19) Bobrick, M. A.; Hodgson, K. O.; Holm, R. H. *Inorg. Chem.* **1977**, *16*, 1851–1858.
(20) Que, L., Jr.; Bobrick, M. A.; Ibers, J. A.; Holm, R. H. *J. Am. Chem. Soc.* **1974**, *96*, 4168–4177.
(21) Haddad, M. S.; Federer, W. D.; Lynch, M. W.; Hendrickson, D. N. *Inorg. Chem.* **1981**, *20*, 131–139.

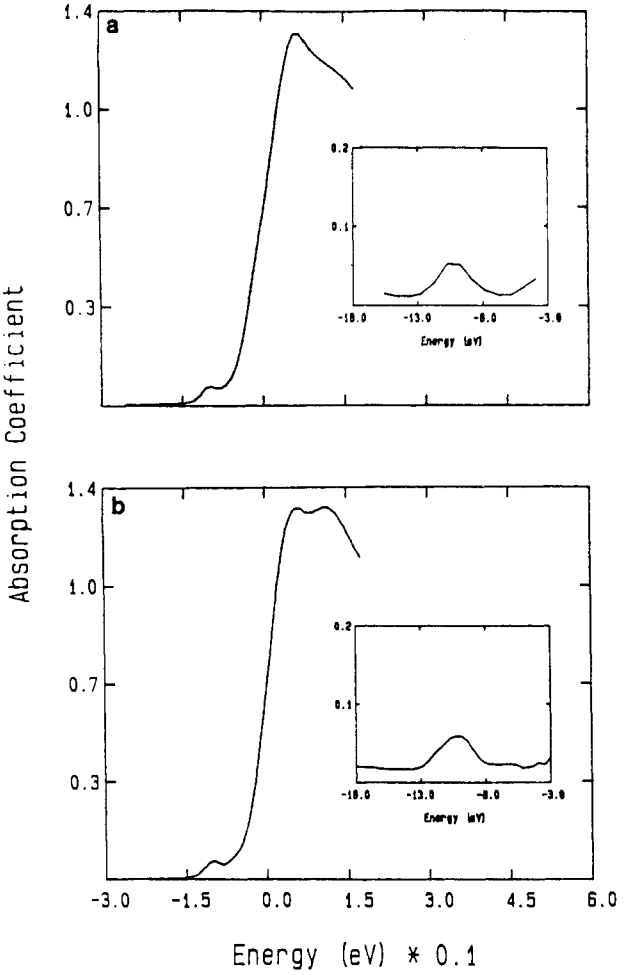

Figure 1. Near-edge XAS spectra of (a) (μ-S)metHr and (b) metHrN$_3$. The inserts are expansions of the background-corrected pre-edge regions.

complex deviates from octahedral symmetry.[15] The edge features of (μ-S)metHr are compared with those of metHrN$_3$ in Figure 1. The area under the pre-edge peak of (μ-S)metHr is indistinguishable from that obtained for metHrN$_3$, indicating that the coordination number of the iron atoms in (μ-S)metHr has not been substantially altered from 6,6 in metHrN$_3$. Given chemical analyses which show that each dinuclear cluster contains one sulfur atom,[12] a total of 9–11 O,N-donors are required to complete the first coordination sphere of the iron atoms. The number of ligands required depends on the presence or absence of a sulfido bridge, the presence or absence of an oxo bridge, and 5,6 or 6,6 coordination numbers for the irons.

B. EXAFS. Analysis of EXAFS spectra using the restricted-fit protocol, where r and σ^2 (or N) are the only two adjustable parameters for an absorber–scatterer pair, has previously been used to obtain structural information about the first three coordination spheres of metHrN$_3$ and semi-metHrN$_3$.[3a] The results of least-squares refinements of Fourier-filtered data for (μ-S)metHr using this procedure are summarized in Table I. Because the parameters obtained from fits of the unfiltered data do not suffer from the truncation errors inherent in the analysis of Fourier-filtered data, parameters obtained from unfiltered data are more reliable. However, a larger number of variables must be refined in order to fit the unfiltered data, and the potential exists for a larger number of correlations between refined parameters. For these reasons, parameters obtained from Fourier-filtered data were used as initial parameters for refinements using unfiltered data. The results of these refinements are summarized in Table II. Comparison of the results obtained from Fourier-filtered (Table I) and unfiltered data (Table II) does not reveal any significant differences in bond lengths or other refined parameters. The data and representative fits by both techniques can be graphically compared in Figures 2–5.

The fits of unfiltered data (Table II) employed five shells of scattering atoms, one of which may be a mixed O,N shell with the values of r and σ^2 for the O-scatterers bound to the adjustable parameters of the N-scatterers (see Experimental Section). The advantage that arises from this approach, which does not have any more adjustable parameters than a single O or N shell, lies in the improved value of the average O,N bond length and in a better estimate of N. A study of structurally characterized model compounds with mixed O,N-donors in the first coordination sphere has indicated that although the EXAFS arising from the O,N-scatterers can be fit with a single shell of either O- or N-scatterers, attempts to do so lead to systematic errors in the average bond length of the first-coordination-sphere scattering atoms and often yield unrea-

Table I. Fits Obtained from Fourier-Filtered EXAFS Data[a]

sample	fit no.	coord sphere	r(Fe–X), pm	adjusted param	R
(μ-S)metHr	1	1	6 N: 208.4 (2)	σ^2 = 55	0.55
	2		O: 182.8 (5) 5N: 208.3 (1)	σ^2 = 32 σ^2 = 53	0.26
	3		5N: 213.3 (4) S: 217.4 (3)	σ^2 = 104 σ^2 = 8	0.37
	4		O: 181.2 (4) 2 O, 3 N: 207.5 (2)	σ^2 = 18 σ^2 = 13	0.38
	5		2 O, 3 N: 214.7 (4) S: 217.9 (2)	σ^2 = 104 σ^2 = 8	0.38
	6	2, 3	C: 319 (1) Fe: 336 (1) C: 433 (1)	N = 4 σ^2 = 55 N = 7	0.39
	7		Fe: 313 (1) C: 338 (1) C: 434 (1)	σ^2 = 68 N = 9 N = 6	0.20
(μ-S)semi-metHr	8	1	6 N: 218.9 (2)	σ^2 = 140	0.54
	9		S: 217.9 (1) 5 N: 223.6 (1)	σ^2 = −11 σ^2 = 18	0.16
	10		S: 216.5 (2) 2 O, 3 N: 222.0 (2)	σ^2 = 5 σ^2 = 13	0.25
	11		2 O, 3 N: 214.0 (4) S: 241.6 (4)	σ^2 = 111 σ^2 = 35	0.40
	12	2, 3	C: 342 (1) Fe: 358 (1) C: 403 (1)	N = 8 σ^2 = 31 N = 9	0.16
	13		Fe: 335 (1) C: 361 (1) C: 404 (1)	σ^2 = 64 N = 7 N = 5	0.32

[a] Coordination spheres 1 and 2, 3 correspond to back-transform windows of 110–230 and 240–410 pm, respectively; values of σ^2 are in units in pm^2.

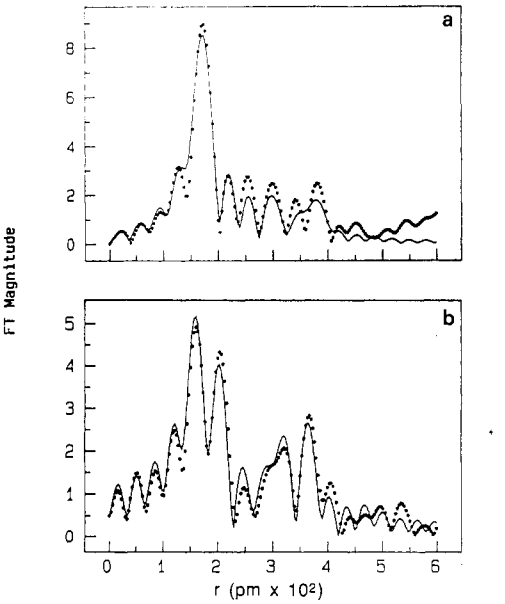

Figure 2. Fourier transforms of EXAFS data (0.04–0.14 pm^{-1}), with dots representing data points and solid lines indicating the Fourier transforms of the multishell fits to the data using identical transform limits: (a) (μ-S)metHr, (b) (μ-S)semi-metHr. The fits shown are from Table II, fits 5 and 13, respectively. The value of r in this figure represents the interatomic distance plus a phase shift.

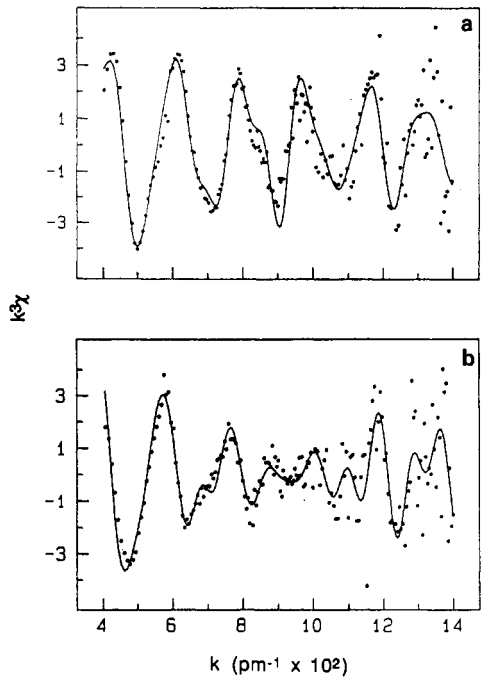

Figure 3. Unfiltered EXAFS data (dots) and multishell fits (solid line): (a) (μ-S)metHr; (b) (μ-S)semi-metHr. The fits shown are from Table II, fits 5 and 13, respectively.

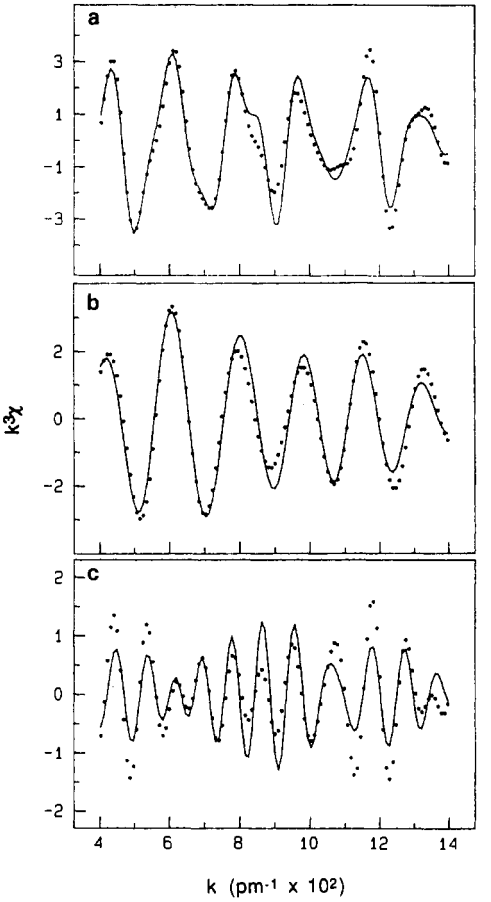

Figure 4. Fourier-filtered data and multishell fits for (μ-S)metHr. Dots represent data points, and the solid line represents the multishell fit (Table II, fit 5), which was Fourier-transformed and back-transformed by using the same limits as the data. Parts a–c represent EXAFS arising from all scattering atoms (110–410 pm), first-coordination-sphere scattering atoms (110–230 pm), and second- and third-coordination-sphere scattering atoms (240–410 pm), respectively.

sonable values of N. These effects can be traced to the presence of interference in the EXAFS arising from O-donors (carboxylates) and

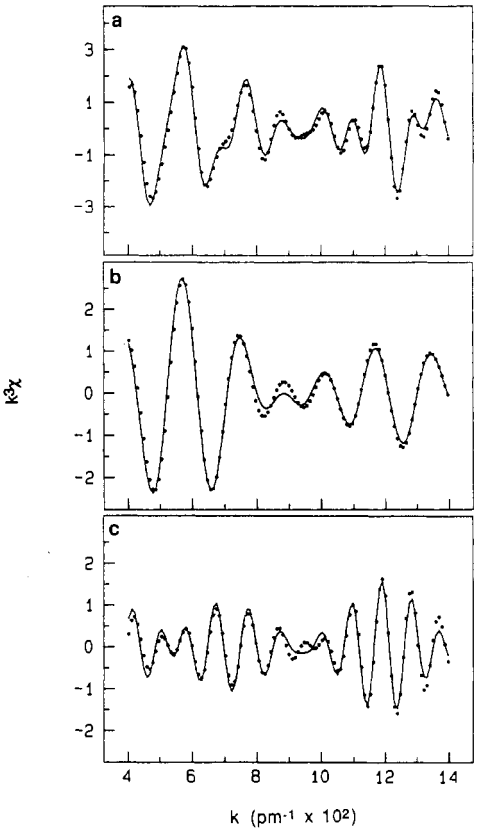

Figure 5. Fourier-filtered data and multishell fits (Table II, fit 13) for (μ-S)semi-metHr. Parts a–c represent EXAFS arising from all scattering atoms, first-coordination-sphere scattering atoms, and second- and third-coordination-sphere scattering atoms, respectively. See Figure 4 for details and back-transform limits.

N-donors (histidines) that feature different, but unresolvable, Fe–L distances.[3a] In the case of (μ-S)metHr, the use of a mixed O,N first shell does not give substantially better (or poorer) quality fits, as judged by the value of R, but does give an adjustment of the average bond length from that obtained with a single N shell (Table II, fits 1 and 2). (Note: The use of a single shell of O-scattering atoms always gave a poorer fit than could be obtained by using a single shell of with the same number of N-scatterers.) These adjustments are in the direction and of the magnitude expected from the study of structurally characterized Hr models.[3a] Further, the use of the mixed N,O shell also significantly lowers the correlation coefficient between this shell and the S-scatterer (Table II, fits 4 and 5). For these reasons, an average O,N bond length of 214 pm for the first coordination sphere is the most reliable result. The use of mixed O,N scatterers in the first coordination sphere also allows a direct comparison with previous fits[3a] of other forms of Hr to be made.

In addition to the O,N shell, one other scattering atom was required to fit the first-coordination-sphere data. The inclusion of a single sulfur scatterer at 218 pm in the presence of five O,N-scatterers at an average distance of 214 pm led to a reasonable fit of the data (Table I, fits 1, 3, and 5; Table II, fits 1, 2, and 5). The best fit was obtained for one sulfur per iron and, given analytical data indicating that one sulfur per dinuclear unit is involved in (μ-S)metHr,[12] a bridging role for the sulfur atom is indicated. The Fe–S distance obtained is also consistent with a sulfido bridge. This distance is comparable to those obtained for bridging sulfide in $[Fe(salen)]_2S$ (217 pm)[22] and in $[Fe_2S_2X_4]^{2-}$ complexes (218–220 pm)[23] and considerably shorter than expected for a terminal SH^- ligand like that found in a ferric porphyrin complex (230 pm).[24]

Further support for a sulfido bridge can be obtained from an analysis of the σ^2 values. Previous fits of oxo-bridged forms of Hr and model

(22) Dorfman, J. R.; Girerd, J.-J.; Simhon, E. D.; Stack, T. D. P.; Holm, R. H. *Inorg. Chem.* **1984**, *23*, 4407–4412.
(23) (a) Coucouvanis, D.; Salifoglou, A.; Kanatzidis, M. G.; Simopoulos, A.; Papaefthymiou, V. *J. Am. Chem. Soc.* **1984**, *106*, 6081–6082. (b) Coucouvanis, D.; Swenson, D.; Stremple, P.; Baenziger, N. C. *J. Am. Chem. Soc.* **1979**, *101*, 3392–3394. (c) Mayerle, J. J.; Denmark, S. E.; De Pamphilis, B. V.; Ibers, J. A.; Holm, R. H. *J. Am. Chem. Soc.* **1975**, *97*, 1032–1045.
(24) English, D. R.; Hendrickson, D. N.; Suslick, K. S. *J. Am. Chem. Soc.* **1984**, *106*, 7258–7259.

Table II: Fits Obtained from Unfiltered EXAFS Data[a]

sample	fit no.	r(Fe–X), pm	adjusted param	R	correln coeff >0.60
(μ-S)metHr	1	5 N: 208.8 (3)	σ^2 = 37	1.14	
	2	5 N: 214.3 (9)	σ^2 = 114	1.08	Fe–S/σ^2(N) = 0.77
		S: 217.7 (5)	σ^2 = 4		
	3	5 N: 214.7 (8)	σ^2 = 109	1.03	Fe–S/σ^2(N) = 0.79
		S: 217.6 (5)	σ^2 = 3		
		C: 316 (2)	N = 4		Fe–C/σ^2(Fe) = –0.65
		Fe: 335 (1)	σ^2 = 85		
	4	5 N: 215.1 (8)	σ^2 = 108	0.94	Fe–S/σ^2(N) = 0.78
		S: 217.5 (4)	σ^2 = 3		
		C: 317 (2)	N = 4		Fe–C/σ^2(Fe) = –0.65
		Fe: 335 (1)	σ^2 = 74		
		C: 433 (1)	N = 7		
	5	2 O, 3 N: 213.8 (8)	σ^2 = 111	0.96	Fe–S/σ^2(O,N) = 0.64
		S: 217.9 (4)	σ^2 = 3		
		C: 317 (2)	N = 4		Fe–C/σ^2(Fe) = –0.66
		Fe: 335 (1)	σ^2 = 75		
		C: 433 (1)	N = 6		
	6	2 O, 3 N: 213.5 (9)	σ^2 = 129	0.99	(Fe–S/σ^2(O,N) = 0.59)
		S: 218.1 (4)	σ^2 = 3		
		Fe: 313 (1)	σ^2 = 99		(Fe–C/σ^2(Fe) = –0.55)
		C: 339 (1)	N = 6		
		C: 433 (2)	N = 5		
(μ-S)semi-metHr	7	5 N: 219 (1)	σ^2 = 128	1.24	
	8	S: 217.7 (5)	σ^2 = –4	1.09	Fe–S/Fe–N = 0.84
		5 N: 223.7 (6)	σ^2 = 25		σ^2(N)/σ^2(S) = 0.86
	9	5 N: 214.6 (8)	σ^2 = 106	1.15	
		S: 241.3 (7)	σ^2 = 25		
	10	S: 217.9 (5)	σ^2 = –4	1.02	Fe–S/Fe–N = 0.84
		5 N: 223.9 (5)	σ^2 = 24		σ^2(N)/σ^2(S) = 0.85
		C: 337 (2)	N = 4		
		Fe: 364 (3)	σ^2 = 150		
	11	S: 218.1 (4)	σ^2 = –7	0.90	Fe–S/Fe–N = 0.84
		5 N: 224.1 (5)	σ^2 = 23		σ^2(N)/σ^2(S) = 0.85
		C: 343 (1)	N = 7		Fe–C/σ^2(Fe) = –0.72
		Fe: 359 (1)	σ^2 = 29		
		C: 403 (1)	N = 9		
	12	5 N: 214.3 (7)	σ^2 = 104	0.98	
		S: 241.2 (6)	σ^2 = 20		
		C: 344 (2)	N = 6.3		Fe–C/σ^2(Fe) = –0.72
		Fe: 360 (1)	σ^2 = 29		σ^2(Fe)/N_C = –0.61
		C: 404 (1)	N = 9.9		
	13	S: 216.7 (5)	σ^2 = 2	0.90	Fe–S/Fe–O,N = 0.81
		2 O, 3 N: 222.3 (5)	σ^2 = 9		σ^2(O,N)/σ^2(S) = 0.80
		C: 343 (1)	N = 7		Fe–C/σ^2(Fe) = –0.70
		Fe: 359 (1)	σ^2 = 29		
		C: 403 (1)	N = 9		
	14	S: 215.5 (4)	σ^2 = 5	0.98	Fe–S/Fe–O,N = 0.74
		2 O, 3 N: 222.5 (5)	σ^2 = 29		σ^2(O,N)/σ^2(S) = 0.79
		Fe: 335 (1)	σ^2 = 72		
		C: 362 (1)	N = 7		
		C: 405 (1)	N = 6		

[a] See Table I for explanation of entries.

compounds employing an identical fitting strategy reveal that the bridging group has an unusually small value of σ^2 associated with it, which was attributed to a decrease in vibrational disorder due to the strong Fe–O–Fe interaction (e.g.: $Fe(acac)_3$, σ^2(O) = 30 pm^2; [((HB-$(pz)_3$)Fe)$_2$O$(OAc)_2$], σ^2(oxo) = 7 pm^2).[3a] The small values of σ^2 obtained for the S-scatterer in fits of (μ-S)metHr are consistent with a similar bridging role (Table II, fit 5; σ^2(S) = 3 pm^2).

The analysis of the first-coordination-sphere data included an examination of the effect of varying the total number of O,N-scatterers over the range of 9–11, the range indicated by pre-edge analysis. Optimum fits, as judged by the value of R, were obtained for a total number of 10 O,N-scatterers, indicating that each iron atom is roughly six-coordinate. Since the electronic absorption spectrum of (μ-S)metHr does not show the pH dependence characteristic of metHr,[13] and given that EXAFS analysis is not expected to be able to distinguish between 6,6 and 5,6 coordination numbers in (μ-S)metHr, the results are consistent with one five-coordinate iron site and one six-coordinate iron site, as found in crystals of metHr.[7a] The average Fe–O,N distance is identical with that obtained previously for metHrN_3,[3a] indicating that little change occurs in the histidine and carboxylate ligation upon exchange of the native oxo bridge for a sulfido bridge.

However, the inclusion of the S-scatterer is not required to generate a satisfactory fit of the data. A fit can also be obtained by including an oxygen scatterer at a short distance (e.g. 181 pm; Table I, fits 2 and 4), like that found in oxo-bridged metHrN_3.[3a] This fit can be rejected because the values of σ^2 from this fit indicate greater disorder for the Fe–oxo distances than for the Fe–O,N distances, which is not expected and not observed for metHrN_3 or any of the dinuclear oxo-bridged models.[3a] Further, while the choice of a sulfido or oxo bridge does not affect the distances found for second- and third-coordination-sphere atoms, it does affect the distances found for other atoms in the first coordination sphere. The inclusion of a short oxygen atom distance leads to an average distance of 208 pm for the remaining O,N shell (Table I, fits 2 and 4). This distance is shorter by 4 pm than that found in other oxo-bridged complexes with three N-donor ligands per iron atom.[3a] When they are taken together, these data argue against the existence of

an oxo bridge in (μ-S)metHr. The reason that fits of the data can be obtained by employing either a sulfido or oxo bridge lies principally in the absence of a distinct beat pattern in the first-coordination-sphere data (Figure 4b). The effect of the S-donor at 218 pm (or O-donor at 181 pm) is mainly one of destructive interference with the five O,N scatterers that comprise the rest of the first-sphere atoms. The inclusion of a sulfur atom in the model is consistent with other physical data on the protein, particularly resonance Raman spectra that feature vibrations associated with bridging sulfur and demonstrate the absence of vibrations associated with an oxo bridge.[12] If a sulfur atom is included, it must have a bond length near that of the O,N-donors in the first coordination sphere or a beat pattern would be expected, such as that exhibited for (μ-S)semi-metHr (Figure 5b, vide infra).

As is the case for other forms of Hr,[3a] three shells of scatterers were used to fit the EXAFS arising from atoms outside the first coordination sphere. Given the dinuclear structure of the site, these correspond to contributions from second-coordination-sphere carbon atoms, the second-coordination-sphere iron atom, and third-coordination-sphere C and N atoms of the histidine ligands. The distances for the second-sphere carbon atoms and iron atom are fairly close, and it is not possible to resolve the two components via Fourier-filtering the data. For this reason, fits for second- and third-sphere atoms from Fourier-filtered data were generated with back-transform windows large enough to accommodate all of the scattering atoms not included in the first coordination sphere. Here again, it is possible to generate two fits to the data (e.g. Table II, fits 5 and 6). The first of these involves an iron atom at 335 pm and carbon atoms at 317 pm. The second fit involves carbon atoms at 339 pm and the iron atom at 313 pm. The distances for the scatterers in the first coordination sphere and the third coordination sphere are not greatly affected by the choice of fits involving differences in the scatterers in the second coordination sphere. It was not possible to distinguish between the Fe and C contributions to the EXAFS by either diminishing the k-weighting of the data or by truncating the data at smaller values of k in performing the Fourier transforms. Although fits obtained by using Fourier-filtered data indicate that a better fit is obtained with a shorter Fe–Fe distance (Table I, fits 6 and 7), this is not the case with unfiltered data (Table II, fits 5 and 6), where the fits are essentially indistinguishable but favor the fit with the longer Fe–Fe distance.

Other criteria were employed in order to elucidate the best fit of the data. For hemerythrin and hemerythrin model compounds, the shorter of the two distances is expected to arise from the Fe–C vector.[3a] This expectation is confirmed in this case by binding the Fe–C distance to the Fe–N distance in multishell fits of the unfiltered data by using a difference of 99.3 pm for the Fe–N and Fe–C distances obtained from a single-crystal X-ray diffraction structural determination of $[Fe(Im)_6](BPh_4)_2$.[25] This procedure gives the fit with the Fe–C distance shorter than the Fe–Fe distance. Further refinement of the Fe–C distances independent of the Fe–N distance leads to fit 5 in Table II, with a corresponding difference of 98 pm. Although this method does not take into account the possibility that histidine ligands may not be symmetrically disposed about the Fe–N bond axis,[26] it appears to work satisfactorily in this case.

The result that the 335-pm distance belongs to the iron scatterer is well within the range of Fe–Fe distances exhibited by oxo/hydroxo-bridged forms of Hr and model compounds[3a] and is additional evidence of only minor changes in the structure of the dinuclear cluster in (μ-S)metHr, except for the bridge. The Fe–Fe distance found is somewhat shorter than that found in semi-metHrN$_3$ (346 pm) but considerably longer than the Fe–Fe distance found for metHrN$_3$ (319 pm).[3a] The difference in Fe–Fe distances between (μ-S)metHr and metHrN$_3$ (16 pm) presumably arises from the increased size of the sulfido bridge compared to that of an oxo bridge. The Fe–Fe distance, along with the longer Fe–S bonds, results in an Fe–S–Fe angle of 100°, assuming a symmetrical bridge. This value is in reasonable agreement with that calculated from resonance Raman vibrational data (ca. 80°).[12] Comparison of this value with the Fe–O–Fe angles calculated from the EXAFS data[3a] for metHrN$_3$ (125°) and semi-metHrN$_3$ (119°) and from the crystal structures of metHr (127°),[7a] metHrN$_3$ (135°),[7a] and metmyoHrN$_3$ (132°)[7b] demonstrate that the μ-sulfido bridging angle is indeed considerably more acute than the bridging angle associated with oxo or hydroxo bridges in Hr. These findings are consistent with expectations from model compounds. In a recent study of dinuclear Fe complexes, where the Fe was bridged by a single oxo or sulfido group, the sulfido-bridged compounds featured smaller bridging angles than the analogous oxo-bridged complexes.[27] The much larger Fe–Fe distances found in these complexes with unsupported bridges (372.2–424.9 pm for μ-S^{2-}; 330.1–355.1 pm for μ-O^{2-})[25] compared with the distance found for (μ-S)metHr (335 pm) strongly suggest that the supporting carboxylate bridges are retained in (μ-S)-metHr.

Inclusion of a shell of carbon scatterers to model Fe–C distances in the second coordination sphere has been demonstrated to result in more accurate Fe–Fe distances.[3a] We have also used single-scattering theory, with parameters from structurally similar model compounds, to account for the scattering from third-shell carbon and nitrogen atoms of histidine ligands, where multiple-scattering effects are certainly involved. This approach is valid only as long as the multiple-scattering pathways are roughly similar in the models and the protein. A shell of carbon scattering atoms at 433 pm adequately models the third-coordination-sphere EXAFS. This distance is identical with that found in metHrN$_3$ and is consistent with only small structural changes in the histidine ligation.

II. (μ-S)semi-metHr. The presence of iron in both the +II and +III oxidation states complicates the analysis of pre-edge features for this sulfide complex of Hr, resulting in very broad features from which no useful information could be extracted. The Fourier-filtered first-coordination-sphere data clearly show the presence of more than one shell of scattering atoms (Figure 5b). In this case, no reasonable fit employing a unique oxygen scatterer was obtained; only a model featuring a S-scatterer would fit the data. Adjustment of the total number of O,N-scattering atoms over the range of 9–11 again resulted in 10 as the optimum, as was the case for (μ-S)metHr.

Comparison of the Fourier transforms of the EXAFS data for (μ-S)metHr and (μ-S)semi-metHr (Figure 2) reveals striking changes in the first-coordination-sphere bond lengths. Good fits are obtained for the data only when the Fe–S distance is considerably *shorter* than the Fe–O,N distance (Table I, fits 10 and 11; Table II, fits 8, 9, 11, and 12). In no case is an alternative fit with a long Fe–S distance and a short Fe–O,N distance comparable. The average Fe–S distance (217 pm) remains essentially unchanged from that found in (μ-S)metHr, but the average Fe–O,N distance found for (μ-S)semi-metHr has lengthened to 222 pm. (Note, however, that the Fe–O,N and Fe–S bond distances are correlated with each other with correlation coefficients of ca. 0.8.) In contrast to the case for (μ-S)metHr, the presence of scattering atoms at distinctly different bond lengths in the first coordination sphere gives rise to a distinct beat pattern in the first-sphere EXAFS data (Figure 5b) and is reflected in a split first-sphere peak in the Fourier-transformed spectrum (Figure 2b). Longer bond lengths for O,N-donors are expected upon reduction of the site, and the distance obtained (222 pm) is similar to the average Fe–N distance in $[Fe(Im)_6](BPh_4)_2$ (221 pm).[25]

Additional evidence for a structural change in (μ-S)semi-metHr is apparent in the second- and third-shell data. As was the case for (μ-S)metHr, scattering from second-coordination-sphere carbon atoms occurs at about the same distance as for the iron scatterer and leads to two possible fits of the data (Table II, fits 13 and 14): one fit with an Fe–Fe distance of 359 pm and an Fe–C distance of 343 pm and one fit with an Fe–Fe distance of 335 pm and an Fe–C distance of 362 pm. However, in this case the value of R is significantly lower for the fit with the longer Fe–Fe distance when either Fourier-filtered (Table I, fits 12 and 13) or unfiltered (Table II, fits 13 and 14) data are used. This fit is also consistent with expectations from model compounds[3a] that the Fe–C distance is shorter than the Fe–Fe distance. Thus, the best fit of the data indicates that the Fe–Fe distance has increased by about 24 pm upon reduction. This Fe–Fe distance is 13 pm longer than the Fe–Fe separation found in semi-metHrN$_3$ (346 pm).[3a] This increase is quite similar to the 16-pm increase associated with the substitution of an oxo bridge by a sulfido bridge in metHr (vide supra). An Fe–Fe separation of 358 pm does not preclude the retention of the bridging carboxylate ligands, as carboxylate bridges have been observed to span a distance of 354 pm in model compounds.[28] Thus, no major change in ligation is required to accommodate the larger Fe–Fe distance.

While the third-coordination-sphere data can be modeled by the parameters employed in the (μ-S)metHr analysis, the average Fe–C,N distance found is much too short (403 pm; Table II, fit 13). Such a result would be expected for attempting to fit third-coordination-sphere histidine scatterers if multiple scattering were not taken into account.[26] The fact that our single-scattering parameters no longer compensate for multiple-scattering effects suggests that the contributions from various multiple-scattering pathways have changed. This result is also reflected to a smaller extent in the second-coordination-sphere Fe–C distances and

(25) Miller, L. L.; Jacobson, R. A.; Chen, Y.-S.; Kurtz, D. M., Jr. *Acta Crystallogr., Sect. C*, in press.
(26) (a) Strange, R. W.; Blackburn, N. J.; Knowles, P. F.; Hasnain, S. S. *J. Am. Chem. Soc.* **1987**, *109*, 7157–7162. (b) Blackburn, N. J.; Strange, R. W.; McFadden, L. M.; Hasnain, S. S. *J. Am. Chem. Soc.* **1987**, *109*, 7162–7170.
(27) Mukherjee, R. N.; Stack, T. D. P.; Holm, R. H. *J. Am. Chem. Soc.* **1988**, *110*, 1850–1861.
(28) Chen, Q.; Lynch, J. B.; Gomez-Romero, P.; Ben-Hussein, A.; Jameson, G. B.; O'Connor, C. J.; Que, L., Jr. *J. Am. Chem. Soc.*, in press.

is consistent with a reorientation of the histidine ligands in (μ-S)semi-metHr.

The fact that the Fe–Fe distance has increased in (μ-S)semi-metHr while the Fe–S distance has not leads to a larger bridging angle in this form. The Fe–S–Fe angle calculated by assuming a symmetrical bridge is 111°. This angle is more comparable to that expected for the hydroxo bridge of semi-metHrN_3. Given the large number of shells employed in fitting the data, the addition of a second S-scattering atom to test for the presence of an unsymmetric sulfido bridge is not warranted. However, given the localized Fe(II,III) valences detected by Mössbauer spectroscopy,[11b] an Fe(III)–S distance shorter than the Fe(II)–S distance is very likely in (μ-S)semi-metHr. Such an asymmetry involving the hydroxo bridge of semi-metHrN_3 has been detected by using EXAFS.[3a] Further, unequal Fe–S distances may in part explain why the symmetric Fe–S–Fe stretching frequency *increases* (by 13 cm^{-1}) when (μ-S)metHr is reduced to (μ-S)semi-metHr,[12] despite the increase in bridge angle calculated from the EXAFS data.

The similarity between the Fe–S bond lengths found for (μ-S)semi-metHr and (μ-S)metHr strongly suggests that the sulfido bridge found in (μ-S)metHr is not protonated upon reduction to (μ-S)semi-metHr, in contrast to what has been observed in various metHr and semi-metHr forms with the native O-donor bridging atom.[3a,9] One effect of changing an oxo bridge to a hydroxo bridge is a dramatic drop in the magnitude of the antiferromagnetic exchange coupling constant, J, between the Fe atoms. It has been noted that the value of J found for (μ-S)semi-metHr is about twice as great as that found for the hydroxo-bridged semi-metHr adducts,[9] a result that would arise if the sulfido bridge were retained in (μ-S)semi-metHr. Also, no D_2O effect is observed on the Fe–S–Fe stretching frequency in (μ-S)semi-metHr.[11a]

Another result that would be expected if the sulfido bridge were not protonated in (μ-S)semi-metHr is that the formal charge on the cluster would be decreased by one unit (2+ → 1+) upon reduction from (μ-S)metHr to (μ-S)semi-metHr. This change in charge on the cluster would not occur when the reduction is either coupled to or followed by the protonation of the bridge, as in the case of the native oxo bridge.[29] The decrease in formal positive charge on the (μ-S)semi-metHr cluster and its resistance to protonation may be chiefly responsible for the enhanced stability of (μ-S)semi-metHr relative to other semi-metHr forms and for its resistance to further reduction. This change in formal charge on the iron cluster could also be responsible for the significantly greater lengthening of the average Fe–O,N bond distance upon reduction of (μ-S)metHr to (μ-S)semi-metHr (8 pm) compared to that observed for the analogous metHrN_3 to semi-metHrN_3 conversion (1 pm).

Two alternative forms of semi-metHr have been distinguished by their EPR spectra and by their redox kinetics.[6a,c] One-electron reduction of metHr results in (semi-met)$_r$Hr, whereas one-electron oxidation of deoxyHr results in (semi-met)$_o$Hr. These two semi-met forms are known to spontaneously interconvert. Pearce et al.[29] have proposed that Fe_1 is the site of reduction when metHr is converted to (semi-met)$_r$Hr and that this reduction triggers the structural changes associated with the (semi-met)$_r$Hr → (semi-met)$_o$Hr conversion. These structural changes were proposed to include an increase in the Fe–Fe distance. Kinetic studies of the reduction of (μ-S)metHr also led to the conclusion that Fe_1 is the site of reduction in forming (μ-S)semi-metHr.[30] The structural changes associated with reduction of (μ-S)metHr to (μ-S)semi-metHr, particularly the increases in Fe–Fe and average Fe–O,N distances, may thus be similar in nature to the changes that occur during reduction of metHr to (semi-met)$_r$Hr and its subsequent interconversion with (semi-met)$_o$Hr. In particular, (μ-S)semi-metHr may have an Fe site structure similar to that of (semi-met)$_o$Hr. In effect, the larger sulfido bridge shifts the (semi-met)$_r$Hr/(semi-met)$_o$Hr equilibrium completely to the (semi-met)$_o$Hr form. In this regard, we note that the initial product upon oxidative loss of sulfide from (μ-S)semi-metHr resembles (semi-met)$_o$Hr rather than (semi-met)$_r$Hr.[13] A kinetic barrier to this interconversion is also apparent.[31]

Conclusions

The analysis of XAS data for (μ-S)metHr leads to a structure not unlike that of metHr. The best bond lengths are represented by fits to the unfiltered data employing five shells of scattering atoms, including a mixed O,N shell (Table II, fit 5). The only significant differences are associated with the replacement of the native oxo bridge by a sulfido bridge, which leads to a larger Fe–Fe distance and a much more acute bridging angle. The XAS results, together with the results from chemical analysis, Mössbauer, NMR, and resonance Raman data, support the structure summarized by **2**.

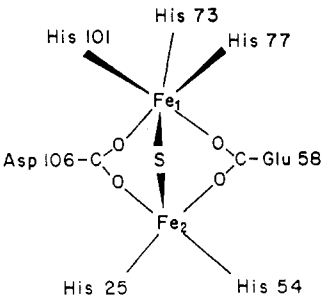

2

In contrast, the EXAFS spectral analysis of (μ-S)semi-metHr data reveals that several structural changes have occurred in the mixed-valent cluster (Table II, fit 13). The average Fe–S bond lengths found in (μ-S)metHr are retained, while the bond lengths associated with histidine and carboxylate ligation increase by 8 pm. These changes are accompanied by an increase in the Fe–Fe distance and a subsequent increase in the Fe–S–Fe angle. These data are consistent with a sulfido bridge, rather than a hydrosulfide bridge, in both forms of the protein. The structural changes found in this work, especially the increase in Fe–Fe distance, upon conversion of (μ-S)metHr to (μ-S)semi-metHr may be similar to conformational changes that occur either during or subsequent to conversion of the corresponding oxo/hydroxo-bridged oxidation levels.

Acknowledgment. This work was supported by Grants NIH-BRSG RR07048 and NIH-GM38829 to M.J.M., NSF-DMB-8314935 and NSF-DMB-8804458 to L.Q., and NIH GM37851 to D.M.K. D.M.K. is an NIH Research Career Development Awardee. R.C.S is grateful for postdoctoral fellowship support from the American Cancer Society. The Cornell High Energy Synchrotron Source is supported by NSF Grant DMR-8412465. The help and guidance of the CHESS staff are gratefully acknowledged.

(29) Pearce, L. L.; Kurtz, D. M., Jr.; Xia, Y.-M.; Debrunner, P. G. *J. Am. Chem. Soc.* **1987**, *109*, 7286–7293.

(30) Pearce, L. L.; Utecht, R. E.; Kurtz, D. M., Jr. *Biochemistry* **1987**, *26*, 8709–8717.

(31) The differing structural motifs of the iron sites in (μ-S)metHr and (μ-S)semi-metHr may be reflected in the two conformers detected in redox titrations of these sulfide derivatives.[13] These conformers have an ~30-mV difference in the met → semi-met midpoint potential. We would associate a higher reduction potential with a protein conformer that favors a longer Fe–Fe distance. Only one conformer was detected in the presence of perchlorate, which was also present in the EXAFS samples.